Liquid Distribution Images on Structured Packing by X-Ray Computed Tomography

P. Marchot, D. Toye, A-M. Pelsser, M. Crine, and G. L'Homme
Laboratoires de Génie Chimique, B6, Université de Liège, Liège B4000, Belgium

Z. Olujic
Laboratory of Process Equipment, Delft University of Technology, 2628CA Delft,The Netherlands

Although distillation is considered to be the most mature among separation technologies, understanding is still inadequate of the processes occurring within a distillation column and, consequently, represents a significant barrier to the further improvement of equipment performance (Adler et al., 1998). In the case of packed columns an obvious barrier for development of advanced predictive models is an inadequate knowledge of the sources and the nature of small-scale liquid and gas maldistributions in packed beds. This obstacle could be overcome if we could see inside the packed bed during operation, that is, develop means to adequately image the liquid flow in a packed bed. X-ray computed tomography is well suited for this purpose, since it is a nonintrusive technique which offers the opportunity to unravel complex flow textures with a sufficient spatial resolution.

The purpose of this article is to present results obtained with the structured packing installed in a column with an internal diameter of 0.6 m, using an air/water system at ambient conditions. Here, we are mainly concerned with the geometric aspect of the problem.

Experimental

The heart of the experimental setup is a 2 m high, 0.6 m internal diameter column made of polyethylene with a wall thickness of 0.015 m. The corrugated sheet structured packing used in this study was Sulzer Mellapak 250 Y made of polypropylene with element/sheet height of 0.31 m. The thickness of corrugated sheets is 1.2 mm, the corrugation height is 0.013 m, and the corrugation base is 0.026 m. The upper and lower 50 mm of the sheet, as well as the central part, are smooth. Two sections in between are rippled and contain a regular pattern of circled and oval holes with a diameter of 6 mm. The height of installed bed consisting of four elements of packing was 1.24 m. Each of these elements consists of two semi-cylindrical segments tightened together by the wall wiper. Water (up to 0.006 m/s) was fed at the top using a liquid distributor with 106 drip points/m^2. Air (up to 2 m/s) was delivered to the bottom of the column by a blower.

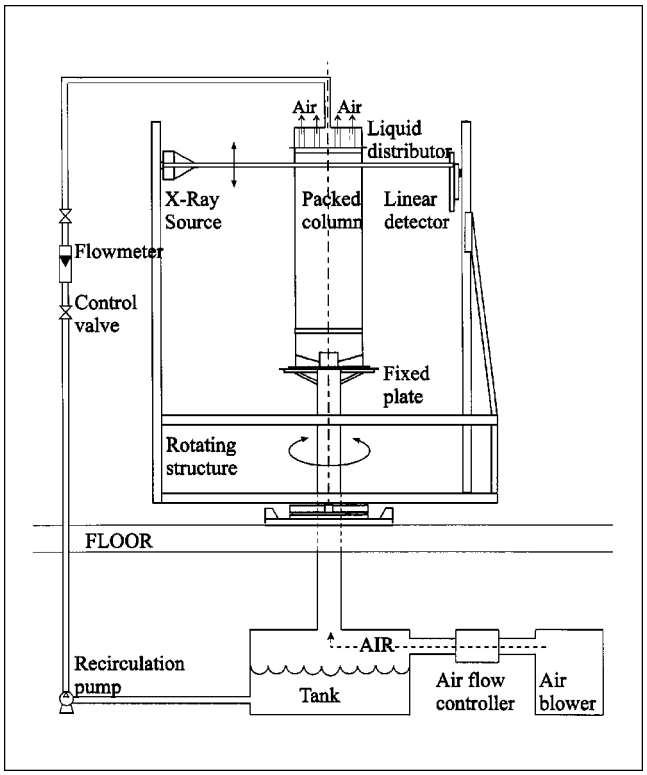

Figure 1. Experimental setup.

Description of the tomograph

We designed a X-ray tomograph (Figure 1) which rotates around a vertical axis giving scans of horizontal sections of a column (Toye et al., 1996). A scan is performed by rotating the source and the detectors continuously at a constant speed

Correspondence concerning this article should be addressed to P. Marchot.

over 360°. The rotation is achieved by a dc motor which is carefully controlled to avoid excessive mechanical strains at startup. The source and the detector bank are fixed on two vertical pillars embedded in a rigid metallic structure. They can be moved vertically by two identical helicoidal screws driven by gears mounted on an horizontal axis rotated by a single dc motor. Vertical position accuracy is 0.001 m. The source provides a collimated flat fan beam of 40° aperture and of 1 mm thickness. We use a focal area of 0.4×0.4 mm and a current of 4 mA, and we operate at 140 kV. The generator is a Baltograph CS160 constant potential, which may be operated between 0−160 kV. The detector bank is a 1.7 m long linear array of 1,024 photodiodes built by Slumberger. A 0.006 m lead sheet is fixed at the back of the bank absorbing the direct radiation. The experimental setup is installed in a dedicated radio protected lab covered by a 0.004 m lead sheet. During a scan, the detector bank sends 1,024 attenuation measures and the angular position every 20 ms through a RS422 port. Signals are fed to the ram of a PC. A scan takes around 160 s leading to files of about 10 Mb. Cross-section images are reconstructed using the linear filtered back projection algorithm. The code is parallelized and runs on a four

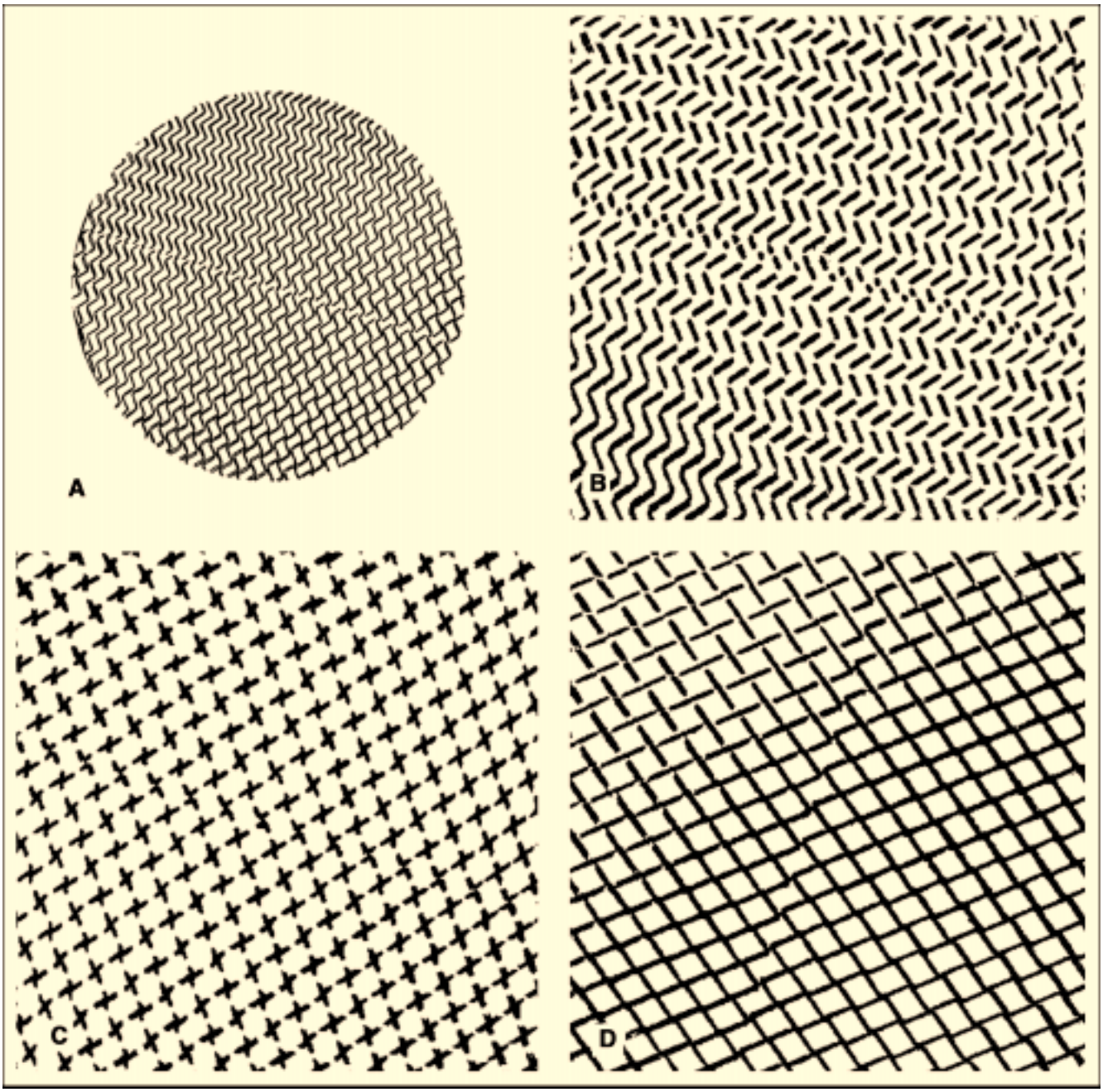

Figure 2. Dry packing.

(A) whole cross section second element from top; (B) first element; (C) first element 32 mm lower than B; (D) fourth element.

processor Sun450. Images of the gas-liquid solid distribution over a grid of 1,024×1,024 pixels are obtained with a resolution around 1 mm.

Procedure

Before beginning an experiment, a blank is realized to set detectors offsets and gains. This setting is valid over a 4 h period. Reconstructed sections are masked, thresholded, and calibrated. Masking is used to remove the column wall image. Noise level is estimated by considering the pixels outside of the mask. A threshold corresponding to 90% of the noise level is applied to the image contained inside the mask. The solid content of the section is obtained by assuming that the maximum pixel value over different scans corresponds to a pixel totally filled by the solid. The dynamic liquid structure is reconstructed by subtracting, before reconstruction, the signals corresponding to the drained column from the signals corresponding to the irrigated column. In order to quantify the dynamic liquid holdup, we determined experimentally the water adsorption coefficient by scanning water samples of known thickness. Then, we computed the ratio of the incident to the transmitted light on the projection signal, without reconstructing the image.

Results

Dry packing

Figures 2a–2d present binarized images of four dry sections taken at various heights. From Figure 2a, which shows a full cross section, it may be clearly seen that a packing element is composed of two semi-cylindrical segments packed tightly to each other. Figures 2b and 2c, which represent a zoom on a square (0.41 m×0.41 m) portion of the cross sectional area taken in the same packing element but vertically separated by 0.032 m, indicate variations of the geometrical structure. Discontinuities in Figure 2b result from the presence of circular holes placed at corrugation ridges. More pronounced discontinuities visible in Figure 2c result from oval holes placed on corrugation sides. Figure 2d presents a very orderly pattern obtained at the position corresponding to the crossings of corrugation sheets. In Figures 2b–2d the split between two cylindrical segments, though still present, is more difficult to distinguish.

The average void fraction measured from such images is 88%, which is the value provided by Sulzer. It fluctuates from section to section, for instance, on the section corresponding to Figure 2c, the void fraction is 90%.

The 2-D autocorrelation function computed on pixel values is used to extract characteristic length from these images (Pratt, 1978). Square images extracted from the cross section are zero padded to 512 pixels. After subtraction of the mean and normalization by the standard deviation, the Fourier transform of the resulting images are computed. The square of their moduli are Fourier inverted then thresholded, leading to binary images of the 2-D autocorrelation function like that shown in Figure 3. The periodic structure of the packing appears clearly and allows the characteristic length to be determined. We obtain d1 = 29.5 pixel and d2 = 39.7 pixel, or d1 = 25 mm and d2 = 34 mm, that is, a 12.5 mm corrugation height (d1/2) and a 24 mm corrugation base length (d2×sin(45°)), which is close to the real values (13 and 26 mm) mentioned earlier.

A closer look into the dry packing structure was taken by performing 18 scans separated vertically by 1mm. These images are assembled in a 3-D data set from which we extract a small volume for visualization. This volume is smoothed by convolution with a 3 pixel wide 3-D box filter. The smoothing makes isosurface determination easier, but leads to an artifi-

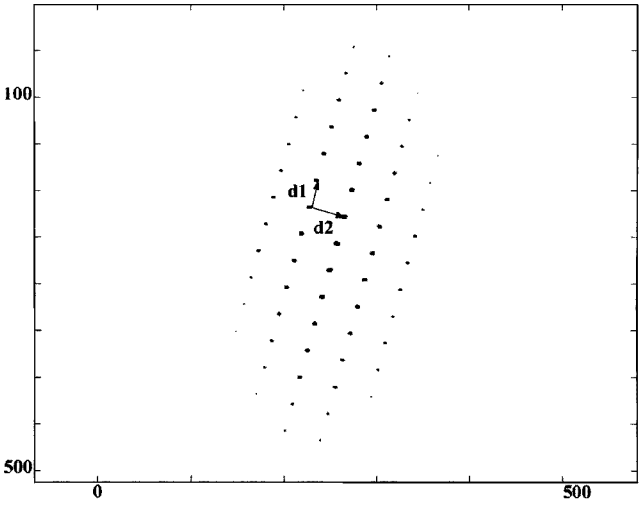

Figure 3. Thresholded autocorrelation function scale in pixel.

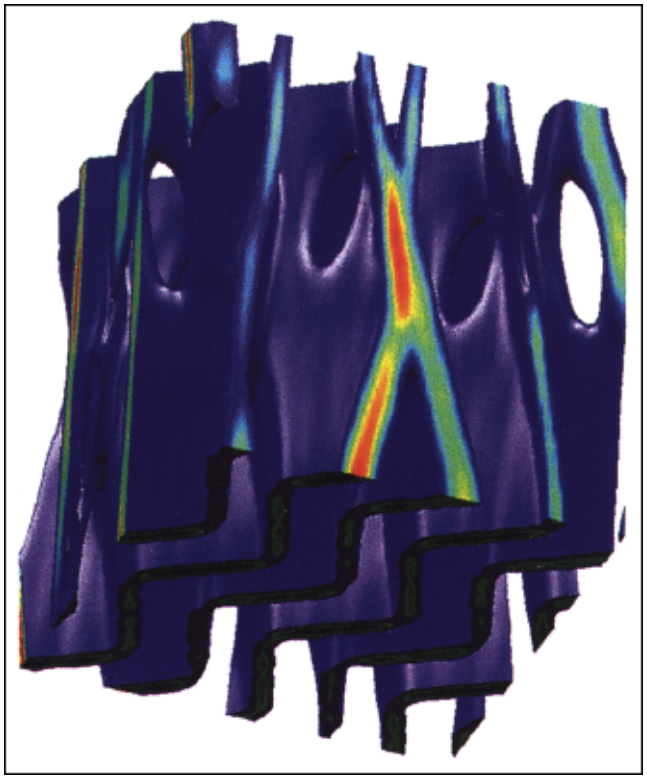

Figure 4. 3-D dry solid packing, 80×80×18 mm.

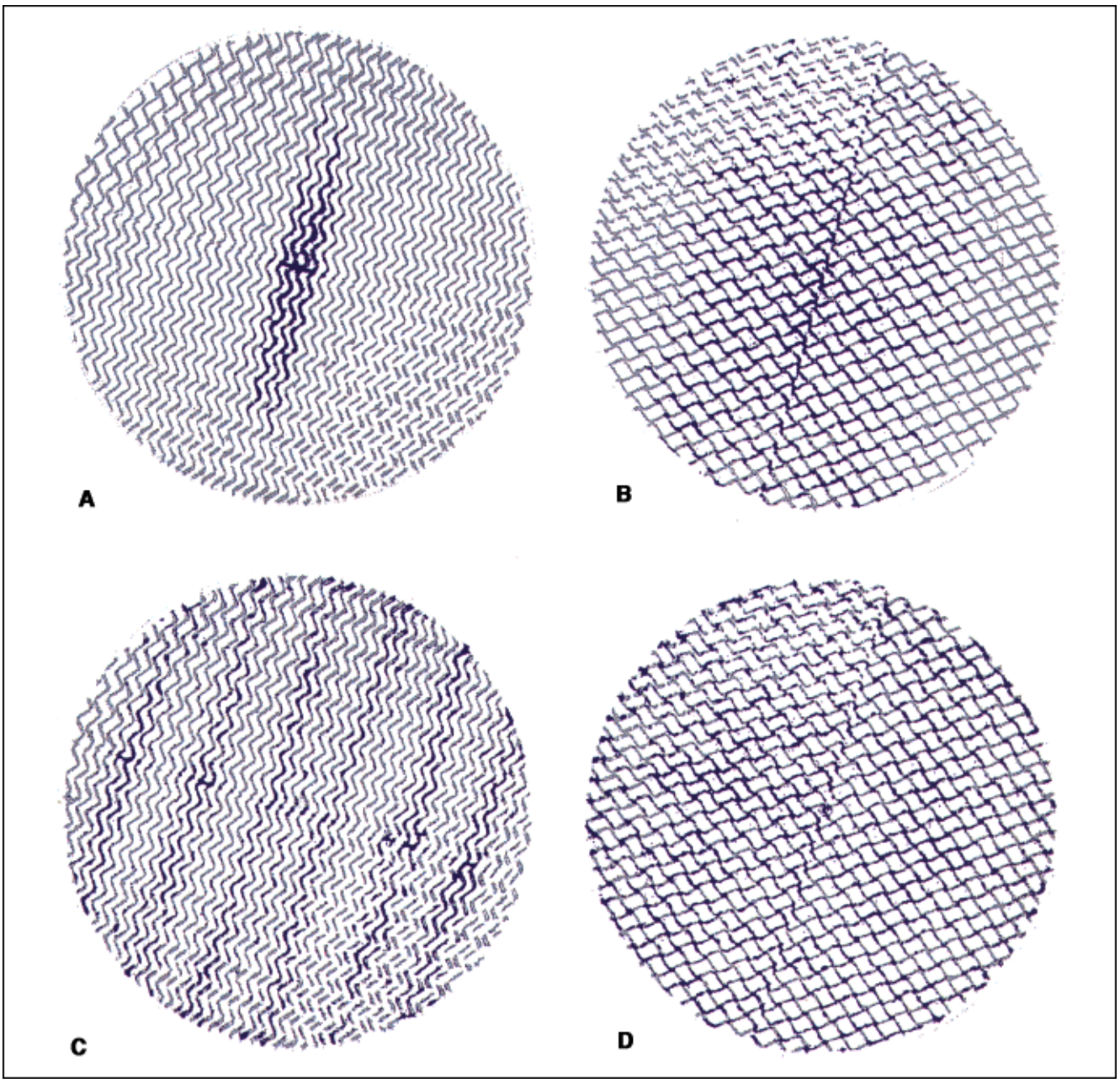

Figure 5. Irrigated packing.

Liquid flow 0.004 m/s. (A) First element, point source; (B) second element, point source; (C) first element, uniform distributor, (D) second element, uniform distributor.

cial increase of the structure thickness. Isosurfaces (surfaces of constant absorption) and isocaps (intersection with the planes delimiting the region of interest) are drawn using Matlab5.3 computing software. Figure 4 represents a 0.018 m $\times$ 0.07 m $\times$ 0.07 m volume extracted from the body of a packing element, indicating corrugations with oval holes. The sheets seem to be fused at their contact points, because their thickness is overestimated by our rather crude image processing.

Irrigated packing

Figures 5A–5D illustrate the dynamic liquid holdup distribution in the packing. They are obtained by superimposing the solid packing image in gray and a thresholded liquid hold-up image in blue. Figures 5A and 5B represent the liquid distribution pattern as observed in a cross section of the first and second packing element, rotated to each other by 90°, resulting from a point source distributor. Figures 5c and 5d represent the same situation for a ''uniform'' (106 drip points/m^2) initial liquid distribution. A slightly thicker blue line indicates increased liquid buildup, which occurs at the location corresponding to the split between two segments of a packing element. This is the first experimental evidence that this kind of structural deviation, causing a discontinuity in the liquid flow, can be considered as a potential source of liquid maldistribution. The possible adverse effect on the

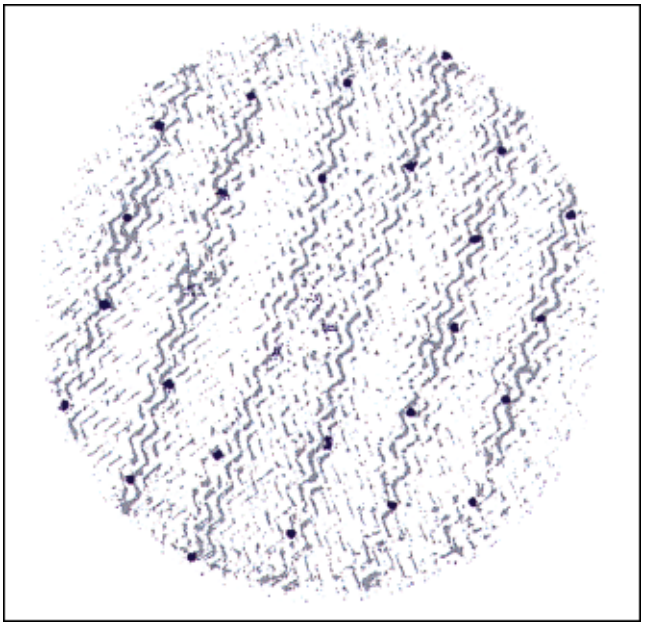

Figure 6. Irrigated packing.

Liquid flow 0.004 m/s. Superposition of the jets flowing from the distributor on the flowing liquid in the first element.

mass-transfer efficiency was considered and modeled by Stoter (1993). Obviously, X-ray tomography, by taking into account the bed layout, provides experimental evidence essential for development and validation of liquid distribution models.

In Figure 6, we superimpose the image of a scan performed through the liquid jets dripping from the distributor in blue to the image of the flowing liquid in a section of the first element in gray. Some of these jets are not properly reconstructed probably because of their fluctuations during the scan. Flowing liquid films or rivulets are detected while notwithstanding their thickness may be less than the pixel size, however, their localization cannot be better than the pixel. Flow patterns like those of Figure 5, were already obtained experimentally by liquid collecting (below the bed) techniques (Hoek et al.,1986) and numerically simulated (Olujic, 1997). They give access to the liquid maldistribution at small, as well as at large, scale. For instance, we measured a strong increase of dynamic liquid holdup at the interface between packing elements. This effect observed by Suess and Spiegel (1992) using the gamma-ray technique, led to a modification of structured packing design (Billingham and Lockett., 1999; Parkinson and Ondrey 1999). Quantitative results about liquid holdup will be presented in another article.

We reconstruct 3-D sections of the flowing liquid following the same procedure used for the dry packing. Figures 7a and 7c represent a 3-D reconstruction of a small portion of the first packing element situated around 0.08 m from the top. Figure 7a shows the dry packing in blue, Figure 7b shows the liquid flowing structure within the same volume, using a uniform distributor, in aquamarine. Superimposing Figures 7a and 7b, we obtain Figure 7c. To get a vivid picture, we choose a volume where the irrigation is poor (which occurs only in the upper part of the first packing element). Due to the

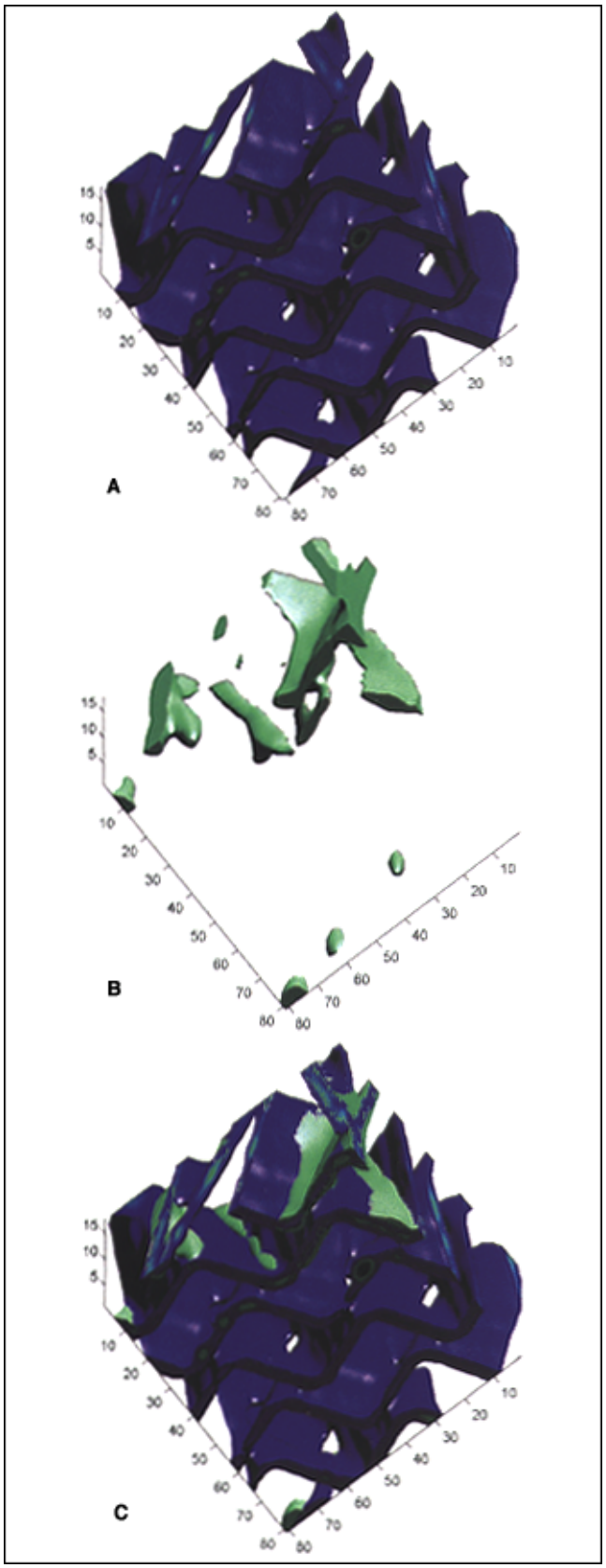

Figure 7. A dry solid, B corresponding flowing liquid structure (first element, liquid flow 0.004 m/s, uniform), C = A + B, axis in mm.

smoothing process used to draw the isosurfaces, structure thickness is increased. This is especially marked for the liquid structure which grows as thick as the solid. Actually, the narrowest smoothing filter we can apply is 3 pixel wide leading nearly inevitably to structures of that thickness. Consequently, it is impossible to ascertain on which side (front or back) of the sheet the liquid is flowing. In spite of their relative geometrical imprecision these pictures are invaluable in small-scale maldistribution investigations.

Conclusions

X-ray computed tomography is a nonintrusive method which provides quantitative information on the small-, as well as on the large-scale liquid maldistribution in any section of a bed consisting of structured packing, essential for development and validation of rigorous predictive models. Very thin flowing liquid structures may be evident and visualized using common 3-D graphic tools. The possibility to locate high liquid hold-up zones might lead to design modification of present commercial structured packings.

Acknowledgment

D. T. is a post-doctoral fellow of the Belgian Fund for Scientific Research (FNRS). Mellapak 250 Y was graciously provided and tailored to our column by Sulzer AG.

Literature Cited

Adler, S., E. Beaver, P. Bryan, J. E. L. Rogers, S. Robinson and C. Russomanno, ''Vision 2020: Separations Roadmap,'' AIChE (1998).

Hoek, P. J., J. A. Wesselingh, and F. J. Zuiderweg, ''Small Scale and Large Scale Liquid Maldistribution in Packed Columns,'' *Chem. Eng. Res. Des.*, **64**, 411 (1986).

Billingham, J. F. and M. J. Lockett, ''Development of a New Generation of Structured Packings for Distillation,'' *Trans IChemE: A*, **77**, 583 (1999).

Olujic, Z., ''Development of a Complete Simulation Model for Predicting the Hydraulic and Separation Performance of Distillation Columns Equipped with Structured Packing,'' *Chem. Biochem. Eng. Q.*, **11**, 31 (1997).

Parkinson, G., and G. Ondrey, ''Packing Towers,'' *Chem. Engineering*, **106**(13), 39 (1999).

Pratt, W. K., *Digital Image Processing*, Wiley, New York, (1978).

Suess, P., and L. Spiegel, ''Hold-up of Mellapak Structured Packings,'' *Chem. Eng. Proc.*, **31**, 119 (1992).

Stoter, C. F., ''Modelling of Maldistribution in Structured Packings: from Detail to Column Design,'' PhD Diss., Delft University of Technology, Delft, The Netherlands (1993).

Toye, D., P. Marchot, M. Crine, and G. L'Homme, ''Modelling of Multiphase Flow in Packed Beds by Computer Assisted X-ray Tomography,'' *Meas. Sci. Technol.*, **7** , 436 (1996).

Manuscript received Apr. 14, 2000, and revision received Oct. 18, 2000.